
NEW MATERIALS, PROCESSES, AND TECHNOLOGIES

Oxidative Dimerization of Methane: Kinetics, Mathematical Modeling, and Optimization with La/Ce Catalysts

**V. A. Makhlin^a, M. V. Podlesnaya^a, A. G. Dedov^b,
A. S. Loktev^b, N. O. Tel'pukhovskaya^b, and I. I. Moiseev^b**

^a Karpov Scientific and Research Institute of Physical Chemistry,
ul. Vorontsovo Pole 10, Moscow, 105064 Russia
e-mail: podlesnaya@bk.ru

^b Gubkin Russian State University of Oil and Gas, Moscow, Russia

Received July 20, 2008

Abstract—Kinetic features of oxidative dimerization of methane to ethane and ethylene, catalyzed by a mixture of lanthanum and cerium oxides deposited onto a magnesium oxide support, were examined. A kinetic model was proposed, and the process optimization was performed for a plug-flow reactor in the quasi-homogeneous approximation.

DOI: 10.1134/S1070363209090333

The world's oil-depletion problem makes natural gas the focus of ever growing attention as an alternative raw material for petrochemical production. Conventionally, methane is converted to liquid hydrocarbons via complex multistage processes. They are run at high pressures and temperatures and entail large capital investments.

In this situation, a good practice will consist in carrying out one-stage conversion of methane to ethylene, in particular, oxidative dimerization of methane at close to atmospheric pressures [1, 2].

Reaction of Oxidative Dimerization of Methane

Considerable researchers' interest in oxidative dimerization of methane is indicated by a huge amount of relevant publications (see, e.g. [1, 3–10]).

In one of the early studies on this subject, Keller and Bhasin [11] described preparation of ethane and ethylene from methane by alternately feeding methane and air onto 5–10% variable-valence metal oxides deposited on Al_2O_3 . With $\text{MnO}/\text{Al}_2\text{O}_3$ and $\text{CdO}/\text{Al}_2\text{O}_3$ catalysts this afforded 10–11% conversion of methane at 800°C with the selectivity of 40–45%. Similar processes catalyzed by oxides capable for oxygen accumulation, e.g., praseodymium [16, 17], terbium

[18], and cerium [19] oxides, were developed by Atlantic Richfield Co. [13, 14] and Union Carbide [16].

Oxidative dimerization of methane in the continuous mode was for the first time carried out with 34% $\text{PbO}/\text{Al}_2\text{O}_3$ [20], 3–7% $\text{Li}_2\text{O}/\text{MgO}$ [21], and rare-earth metal oxides [2] as catalysts. A fairly high yield of C_2 hydrocarbons, 19.6% at the selectivity of 50.3%, was achieved with $\text{Li}_2\text{O}/\text{MgO}$ catalyst [21], and the highest selectivity of 92.8–98.5%, with Sm_2O_3 at 700°C, in which case the methane conversion was 1–5 % [22].

The catalysts most active in oxidative dimerization of methane can be divided into three main groups:

- oxides of *d*- and some *p*-element metals in variable oxidation states, e.g., manganese and lead;
- alkaline and alkali-earth metal oxides;
- rare-earth element oxides.

Also suitable are combinations of these catalysts, in particular, on supports of different nature. For example, products of oxidative dimerization of methane were obtained in 25.8% yield with $\text{SrO}/\text{La}_2\text{O}_3$ catalyst at 800–850°C (selectivity 85.6%) [24], and in 19% yield, with 50% $\text{SrF}_2/\text{Sm}_2\text{O}_3$ catalyst at 800°C (methane

conversion 34%) [25]. In the case of hydroxylapatite the maximal yield of C₂ hydrocarbons (ethylene, ethane) was 22% at 750°C [24].

Bajus and Back [26] suggested active catalysts based on WO₃/ZrO₂ superacids suitable as supports onto which Eu or Ce, together with Li₂CO₃ or, alternatively, Ce or Mn, together with NaCl, were deposited by impregnation. The yield of C₂ hydrocarbons with the first type catalysts was 18%, and the catalysts exhibited stable performance for over 100 h. The second type catalysts provide a higher yield of products but are rapidly deactivated.

For several years oxidative dimerization of methane has been the focus of joint studies by Gubkin Russian State University of Oil and Gas, Karpov Research Physicochemical Institute, Federal State Unitary Enterprise (NIFKhI), and Kurnakov Institute of General and Inorganic Chemistry, Russian Academy of Sciences. The process was catalyzed by rare-earth element oxides synthesized, in particular, from commercial nitrate solutions of rare-earth elements [2, 27–31]. Those studies showed that, by combining lanthanum oxide with cerium oxide, of which the former is catalytically more active in methane dimerization, it is possible to achieve a synergistic effect with respect to the yield of C₂₊ products (ethylene, ethane, propylene, propane). It was also shown that the catalyst comprised of a mixture of La and Ce oxides (9:1 molar ratio), deposited onto molten MgO (periclase), performs efficiently for over 100 h.

Today, there is good reason to be optimistic about the prospects of ethylene preparation by oxidative dimerization of methane. However, choosing the optimal mode and implementation of the process require the knowledge of the kinetic relationships for this reaction.

Kinetic Model of Oxidative Dimerization of Methane

Experimental Technique

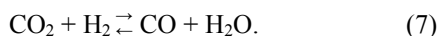
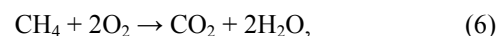
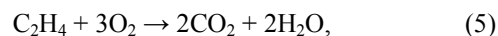
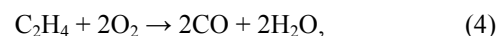
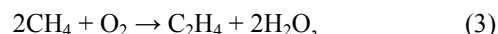
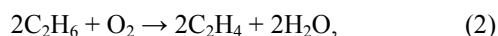
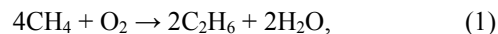
The kinetic examinations were carried out on a laboratory setup comprising a flow reactor. The reactor was designed as a 650×8 mm quartz tube supplied with a mobile thermocouple for measuring the longitudinal temperature profile. A La-Ce/MgO catalyst bed (particle size 0.25–0.50 mm, weighed portion 0.1–0.5 g) was placed into the temperature plateau zone of the reactor. A quartz cotton bed at the reactor inlet, as well as ahead of and after the catalyst bed, served for free

radicals quenching. Such design of the reactor allows minimizing the contribution from gas-phase reactions. The raw materials for the process were found in flow-mixed oxygen and methane (99.999 vol % pure) and methane (99.99 vol % pure, available from Moscow Gas Processing Plant, Open Joint-Stock Company).

The process was run under the following conditions: atmospheric pressure; temperature 700–860°C; methane:oxygen volume ratio 2–7; gas mixture supply rate 1–15 l h⁻¹. The reaction products were identified by chromatomass spectrometry (an Automass-150 chromatomass spectrometer available from Delsi-Nermag, France). Quantitative analysis was carried out by gas-liquid chromatography. The components were separated on three columns (2-m-long), packed with poropack-Q, zeolite NaX, or alumogel modified with sodium carbonate, respectively. A catharometer served as detector, and helium, as carrier gas. The results are summarized in Table 1.

Development of the Kinetic Model of the Process

Table 1 suggests that, under the experimental conditions, the conversion of reactants and selectivity with respect to C₂₊ widely vary. Specifically, the conversion changes from 1 to 35% and from 4 to 98% for methane and oxygen, respectively, and selectivity, from 30 to 70%. The data obtained were described by the following system of stoichiometric equations:



According to this scheme, the kinetic model of the process run in a flow reactor is represented by a system of differential equations describing the rates of consumption of reactants and formation of products in reactions (1)–(7):

$$\frac{dy_{\text{CH}_4}}{d\tau} = -4k_1 \cdot p \cdot \text{CO}_2 - 2k_3 \cdot p \cdot \text{CO}_2 - k_6 \cdot p \cdot \text{CO}_2,$$

$$\frac{dy_{\text{O}_2}}{d\tau} = -k_1 \cdot p \cdot \text{CO}_2 - k_2 \cdot p^2 \cdot \text{CO}_2 \cdot \text{CC}_2\text{H}_6 - k_3 \cdot p \cdot \text{CO}_2 - 2k_4 \cdot p^2 \cdot \text{CO}_2 \cdot \text{CC}_2\text{H}_4 - 3k_5 \cdot p^2 \cdot \text{CO}_2 \cdot \text{CC}_2\text{H}_4 - 2k_6 \cdot p \cdot \text{CO}_2,$$

$$\frac{dy_{\text{C}_2\text{H}_4}}{d\tau} = 2k_2 \cdot p^2 \cdot \text{CO}_2 \cdot \text{CC}_2\text{H}_6 + k_3 \cdot p \cdot \text{CO}_2 - k_4 \cdot p^2 \cdot \text{CO}_2 \cdot \text{CC}_2\text{H}_4 - k_5 \cdot p^2 \cdot \text{CO}_2 \cdot \text{CC}_2\text{H}_4,$$

Table 1. Results of kinetic examinations of oxidative dimerization of methane

Exp. no.	CH ₄ /O ₂	t, °C	Supplied, ml h ⁻¹			Obtained, ml h ⁻¹									
			CH ₄	O ₂	N ₂	CH ₄	C ₂ H ₄	C ₂ H ₆	N ₂	C ₃ H ₆	C ₃ H ₈	CO ₂	CO	O ₂	H ₂
1	3.6	716	13577	3771	43	13352	4	33	43	0	0	91	60	3641	139
2	3.6	790	13427	3730	42	12716	24	148	42	0	4	237	118	3168	216
3	5.3	790	13244	2499	46	12689	19	136	46	0	4	158	75	2115	163
4	3.4	800	8242	2424	43	7562	36	117	43	2	2	243	119	2095	178
5	3.4	838	10107	2973	55	8673	154	227	55	8	10	433	185	1845	68
6	3.4	855	9153	2692	50	7700	181	213	50	14	9	406	190	1535	170
7	2.9	806	2325	802	47	1992	33	30	47	2	1	123	75	423	74
8	2.9	810	2299	793	48	1990	29	28	48	2	1	115	71	451	71
9	2.9	818	2328	803	50	1947	43	30	50	3	1	135	88	370	75
10	3	830	2335	778	42	1868	71	29	42	4	1	171	81	269	78
11	3	840	2310	770	49	1822	71	28	49	4	1	165	110	219	86
12	3	844	2349	783	49	1830	81	28	49	4	1	171	115	178	90
13	3.8	829	2379	626	53	1987	59	31	53	3	1	113	87	220	76
14	3.8	833	2377	626	52	1968	64	31	52	3	1	118	89	213	77
15	3.8	837	2367	623	52	1958	66	31	52	3	1	113	90	203	77
16	3.8	841	2440	642	53	2010	71	31	53	3	1	119	95	193	80
17	1.9	855	1951	1027	128	1343	81	39	128	5	1	294	56	29	58
18	2.1	849	2008	956	118	1400	86	31	118	4	1	312	47	29	58
19	2.9	786	1995	688	77	1519	41	44	77	2	3	241	50	83	72
20	2.9	807	2091	721	73	1561	59	51	73	3	2	270	25	19	65
21	2.9	824	2029	700	168	1521	61	39	168	3	2	253	40	39	59
22	3.6	740	1238	344	44	1163	4	10	44	0	0	36	11	274	26
23	3.6	761	1256	349	50	1172	5	11	50	0	0	38	14	286	27
24	3.4	794	1109	326	75	1002	12	11	75	1	0	46	12	259	27
25	3.4	797	1162	342	55	1030	16	11	55	1	0	52	23	163	29
26	4.4	798	2009	457	49	1824	21	23	49	2	1	65	23	273	42
27	4.4	845	1957	445	48	1699	46	21	48	2	0	86	32	144	49
28	6.9	798	3821	554	46	3632	15	51	46	0	0	46	11	408	45
29	6.9	784	3776	547	44	3673	4	27	44	0	0	33	8	433	39
30	6.9	820	3817	553	47	3592	25	48	47	1	1	59	14	338	49
31	6.9	830	3828	555	65	3590	29	48	65	2	1	60	15	323	50
32	6.9	852	4010	581	47	3674	56	56	47	3	1	79	21	246	64
33	5.1	735	4436	870	48	4373	2	12	48	0	0	31	4	784	15

Table 1. (Contd.)

Exp. no.	CH ₄ /O ₂	t, °C	Supplied, ml h ⁻¹			Obtained, ml h ⁻¹									
			CH ₄	O ₂	N ₂	CH ₄	C ₂ H ₄	C ₂ H ₆	N ₂	C ₃ H ₆	C ₃ H ₈	CO ₂	CO	O ₂	H ₂
34	5.9	750	4297	728	47	4220	3	15	47	1	0	33	5	727	35
35	5.9	796	3827	649	46	3640	16	38	46	0	0	63	16	573	52
36	5.9	860	3597	610	51	3179	76	49	51	5	1	105	45	306	76

$$\frac{dy_{C_2H_6}}{d\tau} = 2k_1 \cdot p \cdot CO_2 - 2k_2 \cdot p^2 \cdot CO_2 \cdot CC_2H_6,$$

$$\frac{dy_{CO_2}}{d\tau} = 2k_5 \cdot p^2 \cdot CO_2 \cdot CC_2H_4 + k_6 \cdot p \cdot CO_2 - k_7 \cdot p^2 \cdot CO_2 \cdot CH_2$$

$$\times \left[1 - \frac{C_{CO} \cdot CH_2O}{K_7 \cdot CCO_2 \cdot CH_2} \right],$$

$$\frac{dy_{CO}}{d\tau} = 2k_4 \cdot p^2 \cdot CC_2H_4 \cdot CO_2 + 2k_7 \cdot p^2 \cdot CCO_2 \cdot CH_2$$

$$\times \left[1 - \frac{C_{CO} \cdot CH_2O}{K_7 \cdot CCO_2 \cdot CH_2} \right],$$

$$\frac{dy_{H_2}}{d\tau} = -k_7 \cdot p^2 \cdot CCO_2 \cdot CH_2 \times \left[1 - \frac{C_{CO} \cdot CH_2O}{K_7 \cdot CCO_2 \cdot CH_2} \right],$$

$$\frac{dy_{O_2}}{d\tau} = 2k_1 \cdot p \cdot CO_2 + 2k_2 \cdot p^2 \cdot CO_2 \cdot CC_2H_6 + 2k_3 \cdot p \cdot CO_2$$

$$+ 2k_4 \cdot p^2 \cdot CO_2 \cdot CC_2H_4 + 2k_5 \cdot p^2 \cdot CO_2 \cdot CC_2H_4 + 2k_6 \cdot p \cdot CO_2$$

$$+ k_7 \cdot p^2 \cdot CCO_2 \cdot CH_2$$

$$\times \left[1 - \frac{C_{CO} \cdot CH_2O}{K_7 \cdot CCO_2 \cdot CH_2} \right],$$

where τ is the conditional contact time; $y_i = W_i/W_0$, conditional proportion of i th component in the flux [W_0 and W_i are the total flux at the reactor inlet and the flux of i th component, $\text{ml h}^{-1} \text{ g}^{-1}$, respectively; p , total pressure in the system, atm; $C_i = y_i/\sum y_i$, mole fraction of i th component in the system; k_j , rate constant of j th reaction; and K_7 , equilibrium constant of reversible reaction (7)].

We determined the numerical values of the Arrhenius parameters to be used for calculating the reaction rate constants ($\ln k_i = A_i + E_i/RT$) in terms of the kinetic model of the process. This was done by minimizing the sum of squared deviations of the experimental and calculated values of the output–input flux differences in the reactor by the Davidon–Fletcher–Powell method [32].

This yielded the following data:

A_i	E_i/R
k_1	-11890
k_2	-9950
k_3	-20000
k_4	-2000
k_5	-10050
k_6	-18870
k_7	-2000

The average relative errors in description of the output–input flux differences were estimated at 32.3, 24.4, 35.9, 49.5, 34.3, and 48.1 for CH₄, O₂, C₂H₄, C₂H₆, CO₂, and CO, respectively.

Mathematical Modeling and Theoretical Optimization of the Process

In terms of the kinetic model developed, mathematical modeling and theoretical optimization in the quasihomogeneous approximation were carried out for oxidative dimerization of methane in a plug-flow reactor. The oxygen conversion and the ethane and ethylene formation selectivity were examined in relation to the conditional time of contact, temperature, pressure, and volume ratio of reactants. The system of differential equations of the kinetic model was solved using the DLSODE program. It is conventionally employed for finding solution to the Cauchy problem in the case of integration of rigid systems of ordinary differential equations by Gear's method [33].

Oxygen Conversion in Relation to the Contact Time of Reactants and Temperature

In commercial application, there will be the need in methane recycling in the process. In this connection, it seemed important to estimate the conditional time of contact that affords high oxygen conversions. Figure 1 presents the plot of oxygen conversion vs. time of contact at a constant volume ratio of reactants (3:1), pressure of 0.1 MPa, and different temperatures. Deep

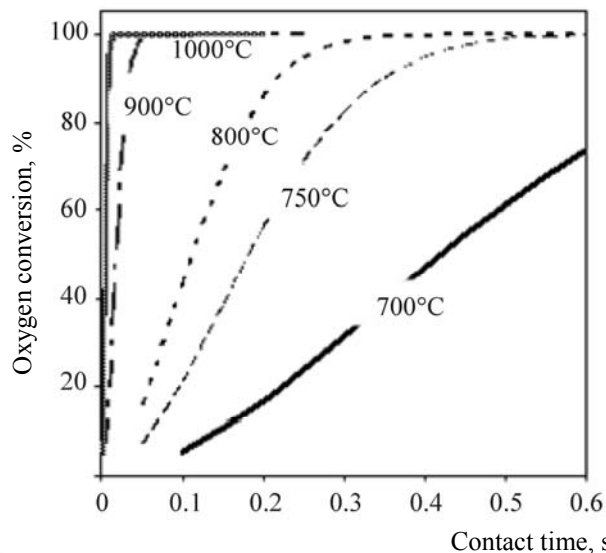


Fig. 1. Oxygen conversion vs. contact time of reactants at different temperatures; $p = 0.1 \text{ MPa}$, $\text{CH}_4:\text{O}_2 = 3:1$.

oxygen conversions ($\geq 95\%$) are achieved at 700°C within 0.9 s, and with temperature increasing to 1000°C the contact time decreases to 0.009 s.

Oxygen Conversion in Relation to Pressure

Commercial application of the process will require maintaining certain excessive pressure in the reactor. Therefore, we examined the main parameters of the process in relation to this pressure. Figure 2 presents the plots of oxygen conversion vs. time of contact at the pressure of 0.17 MPa. Comparison of Figs. 1 and 2 shows that, with increasing pressure, the time of

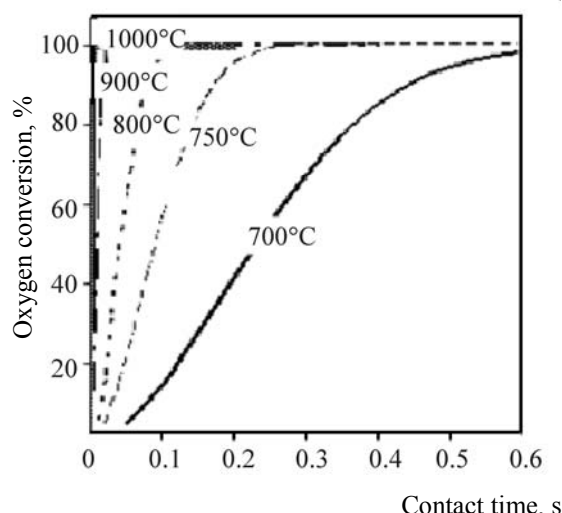


Fig. 2. Oxygen conversion vs. contact time of reactants at different temperatures; $p = 17 \text{ MPa}$, $\text{CH}_4:\text{O}_2 = 3:1$.

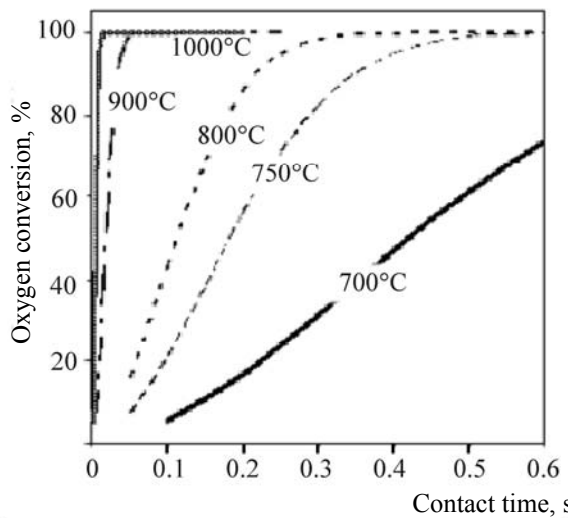


Fig. 3. Oxygen conversion vs. contact time of reactants at different temperatures; $p = 0.1 \text{ MPa}$, $\text{CH}_4:\text{O}_2 = 6:1$.

contact required for achievement of the same oxygen conversion tends to decrease. For example, at the pressure of 0.1 MPa and temperature of 700°C exhaustive oxygen conversion is achieved within 0.9 s, and at the pressure of 0.17 MPa and the same temperature the time of contact is 0.5 s.

Oxygen Conversion in Relation to Reactant Ratio

Comparison of the plots of oxygen conversion vs. time of contact at different temperatures and reactant ratios of 3:1 (Fig. 1) and 6:1 (Fig. 3) suggests that, with increasing $\text{CH}_4:\text{O}_2$ ratio, the time required for exhaustive oxygen conversion tends to decrease. At 800°C and reactant ratio of 3:1 this time was estimated at 0.25 s, and at the 6:1 ratio, at 0.18 s.

Reaction Selectivity in Relation to Oxygen Conversion and Temperature

Figure 4a presents the plot of the reaction selectivity with respect to ethane+ethylene vs. oxygen conversion at different temperatures. It is seen that, with increasing oxygen conversion, the selectivity of the process tends to decrease, but the temperature dependence exhibits a complex pattern. With increasing temperature to 800°C the selectivity of the process tends initially to decrease and subsequently, to increase. To better understand the nature of this dependence, we presented the modeled data on the selectivity-temperature phase plane at three conversion levels, 20, 55, and 95% (Fig. 4b). The resulting plots suggest that the temperature dependence of the selectivity with respect to ethane-ethylene mixture exhibits a pronounced

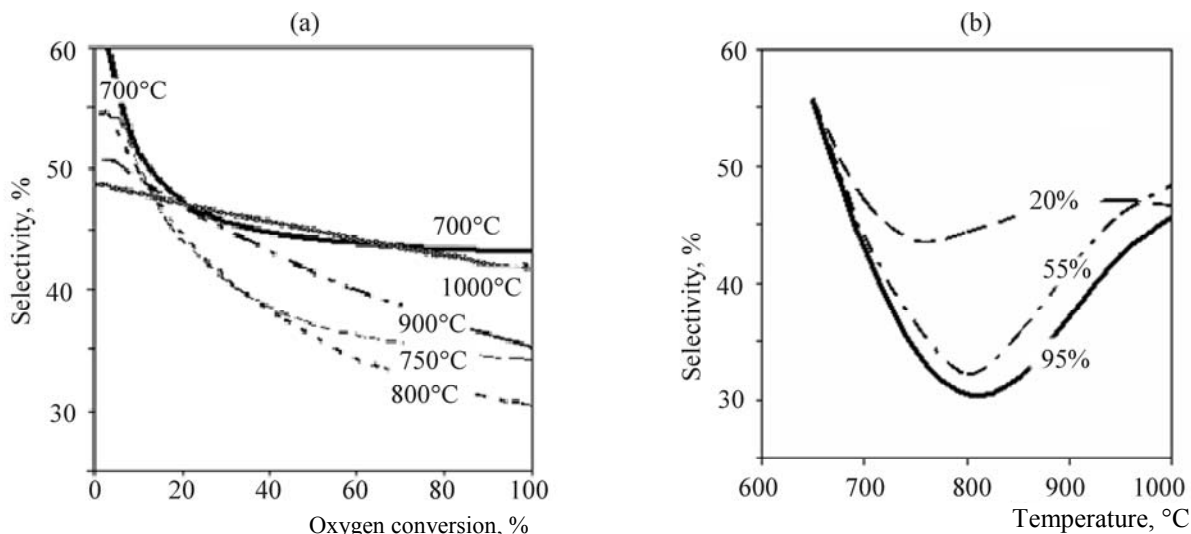


Fig. 4. Process selectivity with respect to ethane-ethylene mixture vs. (a) oxygen conversion at different temperatures and (b) temperature at different oxygen conversions; $p = 0.1$ MPa, $\text{CH}_4:\text{O}_2 = 3:1$.

minimum. For example, at 95% oxygen conversion the minimal selectivity, 30.4%, is observed at 800°C. With decreasing oxygen conversion the minimum is smoothed.

To identify the factors responsible for such unusual temperature dependence of the C_2 product formation selectivity, we plotted the temperature dependences of the selectivity for each individual target product, ethane and ethylene (Fig. 5). It is seen that, over the

temperature range examined, the selectivities exhibit opposite trends, which is responsible for a minimum observed in the plot of the total selectivity.

Reaction Selectivity in Relation to Pressure and Reactant Ratio

Comparison of the temperature dependences of the process selectivity with respect to ethane-ethylene mixture (3:1 volume ratio of reactants) at different pressures (see Figs. 4b and 6) shows that, with

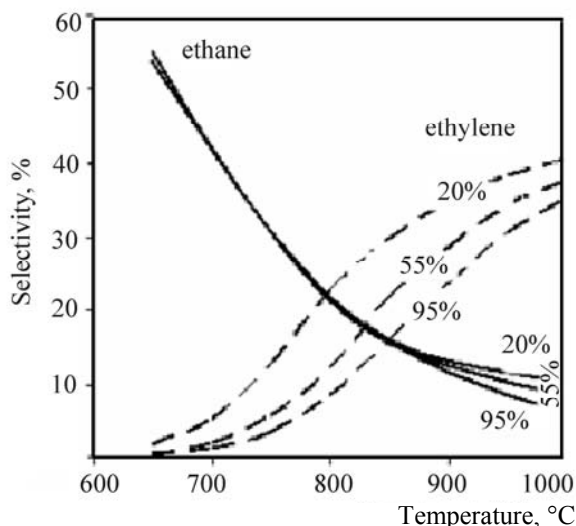


Fig. 5. Process selectivity with respect to ethane and ethylene vs. temperature at different oxygen conversions; $p = 0.1$ MPa, $\text{CH}_4:\text{O}_2 = 3:1$.

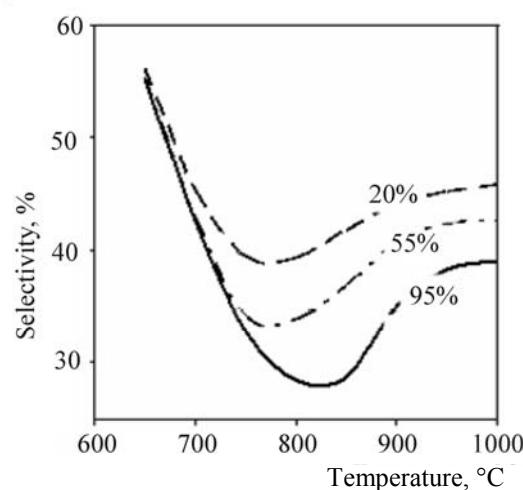


Fig. 6. Temperature dependence of the reaction selectivity with respect to ethane-ethylene mixture at different oxygen conversions; $p = 0.17$ MPa.

Table 2. Results of theoretical optimization of oxidative dimerization of methane

p , atm	CH ₄ :O ₂ , vol %	t , °C	95% O ₂ conversion time, s	Reaction selectivity, %, with respect to indicated products	
				at C ₂ H ₄ + C ₂ H ₆ , %	at C ₂ H ₄ , %
1.0	3:1	700	0.9000	43.06	1.30
		800	0.2500	30.40	8.50
		1000	0.0090	45.60	35.26
		700	0.5000	42.52	0.77
1.7	3:1	800	0.0900	28.40	5.24
		1000	0.0035	39.00	31.56
		700	0.6500	43.94	2.20
1.0	6:1	800	0.1800	35.94	13.02
		1000	0.0100	44.48	38.06

increasing pressure, the selectivity of formation of the ethane-ethylene mixture tends to slightly decrease.

With increasing volume ratio of reactants the selectivity of the process tends to slightly increase: At 3:1 ratio the minimal selectivity is 30.4%, and at 6:1 ratio, 36.0 % (cf. Figs. 4b and 7).

Theoretical optimization of oxidative dimerization of methane (Table 2) revealed the parameter ranges corresponding to the maximal selectivity of the process with respect to C₂ products:

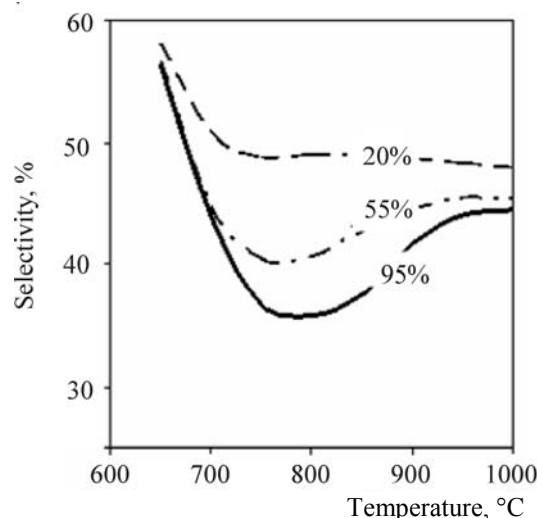


Fig. 7. Temperature dependence of the reaction selectivity with respect to ethane-ethylene mixture at different oxygen conversions; CH₄:O₂ = 6:1.

- (1) low-temperature area 700–750°C,
- (2) high-temperature area 850–950°C.

The optimal pressure was estimated at 1.0–1.7 ata, which is close to atmospheric pressure. Increase in pressure is undesirable because this causes the selectivity to decrease. The optimal volume ratio of reactants CH₄:O₂ is within 3:1–6:1. Increase in the ratio is beneficial for selectivity but increases the recycle of methane. At the same time, the time of contact that affords 95% oxygen conversion is 0.4–0.9 s in the low-temperature area, and 0.02–0.125 s, in the high-temperature area. This fact should also be taken into account when choosing the best conditions, since the time of contact decides the specific yield of the catalyst, all other conditions being the same.

ACKNOWLEDGMENTS

This study was financially supported by the Program of Presidium of the Russian Academy of Sciences no. 7 “Fundamental Problems of Power Engineering” (Subprogram “Theoretical Principles of the Technology of Motor Fuels and Basic Oil Products from Non-Oil Raw Materials”), Russian Foundation for Basic Research (project nos. 07-03-00533-a and 07-03-12039-ofi), and grant of the President of the Russian Federation to support leading scientific schools of the Russian Federation (Academician I.I. Moiseev’s scientific school).

The authors are grateful to A.G. Zyskin, Cand. Sci. (Phys.-Math.), for providing consultancy on the calculations and for discussions on this study.

REFERENCES

1. Krylov, O.V. and Arutyunov, V.S., *Okislitel'nye prevrashcheniya metana* (Oxidative Transformations of Methane), Moscow: Nauka, 1998.
2. Dedov, A.G., Loktev, A.S., Moiseev, I.I., Men'shchikov, V.A., Filimonov, I.N., and Parkhomenko, K.V., *Khim. Prom-st'. Segodnya*, 2003, no. 3, p. 12.
3. Fox, J.M., *Catal. Rev.-Sci. Eng.*, 1993, vol. 35, no. 2, p. 169.
4. Lunsford, J.H., *Angew. Chem. Intern. Ed.*, 1995, vol. 34, no. 9, p. 970.
5. Sokolovskii, V.D., *Catal. Rev.-Sci. Eng.*, 1990, vol. 32, nos. 1–2, p. 1.
6. Hutchings, G.J., Scurrell, M.S., and Woodhouse, J.R., *Chem. Soc. Rev.*, 1989, vol. 18, p. 251.
7. Amenomiya, Y., Birs, V.I., Goledzinowski, M., et al., *Catal. Rev.-Sci. Eng.*, 1990, vol. 32, no. 3, p. 163.
8. Pratt, S., Wiley, D.B., and Harris, I.R., *Platinum Met. Rev.*, 1999, vol. 43, no. 2, p. 50.
9. Lunsford, J.H., *Catal. Today*, 2000, vol. 63, p. 165.
10. Arutyunov, V.S. and Krylov, O.V., *Usp. Khim.*, 2005, vol. 74, no. 12, p. 1237.
11. Keller, G.F. and Bhasin, M.M., *J. Catal.*, 1982, vol. 73, no. 1, p. 9.
12. Sofranko, J.A., Leonard, J.L., and Jones, C.A., *J. Catal.*, 1987, vol. 103, no. 2, p. 302.
13. Gaffney, A.M., Jones, C.A., Leonard, J.L., and Sofranko, J.A., *J. Catal.*, 1988, vol. 114, no. 2, p. 422.
14. Haggins, J., *Chem. Eng. News*, 1988, no. 27, p. 22.
15. US Patent 4499323.
16. US Patent 4727211.
17. US Patent 4727212.
18. US Patent 4499324.
19. Hinsen, W., Bytin, W., and Baerns, M., Abstracts of Papers, *Proc. VIII Int. Congr. on Catalysis*, West Berlin, 1984, Basel: Weinheim, 1984, vol. 3, p. 581.
20. Ito, T. and Lunsford, J.H., *Nature*, 1985, vol. 314, no. 6013, p. 721.
21. Otsuka, K., Jinno, K., and Morikava, A., *J. Catal.*, 1986, vol. 100, p. 353.
22. Yu, L., Li, W., Martin, G.A., Mirodatos, C., and Du-carme, V., *Appl. Catal. A*, 1998, vol. 175, p. 173.
23. Choudhary, V.R., Mulla, S.A.R., and Uphade, B. S., *Fuel*, 1999, vol. 4, p. 427.
24. Machocki, A. and Denis, A., Abstract of Papers, *Proc. 5th Int. Natural Gas Conversion Symp.*, Giardini-Naxos (Sicily), 1998, vol. 119, p. 313.
25. Bajus, M. and Back, M.H., Abstracts of Papers, *Proc. 5th Int. Natural Gas Conversion Symp.*, Giardini-Naxos (Sicily), 1998, vol. 119, p. 289.
26. RF Patent 2134675.
27. Dedov, A.G., Loktev, A.S., Men'shchikov, V.A., Kartasheva, M.N., Parkhomenko, K.V., and Moiseev, I.I., *Dokl. Ross. Akad. Nauk*, 2001, vol. 380, no. 6, p. 791.
28. Dedov, A.G., Loktev, A.S., Men'shchikov, V.A., Parkhomenko, K.V., Lyakishev, G.G., and Moiseev, I.I., *Khim. Tekhnol.*, 2003, no. 4, p. 5.
29. Makhlin, V.A., Dedov, A.G., Loktev, A.S., Parkhomenko, K.V., Tel'pukhovskaya, N.O., Evenchik, A.S., and Moiseev, I.I., *Khim. Tekhnol.*, 2006, no. 7, p. 29.
30. Dedov, A.G., Loktev, A.S., Moiseev, I.I., Aboukais, A., Lamontier, J.-F., and Filimonov, I.N., *Appl. Catal. A*, 2003, vol. 245, p. 209.
31. Fletcher, R. and Powel, M., *Computer Journal*, 1963, vol. 6, no. 2, p. 163.
32. Gear, C.W., *Numerical Initial Value Problems in Ordinary Differential Equations*, New York: Prentice-Hall, Englewood Cliffs, 1971.